JOURNAL OF MATERIALS SCIENCE 19 (1984) 1251–1260

Effect of cold rolling on the superconducting and electronic properties of two amorphous alloys; $Nb_{50}Zr_{35}Si_{15}$ and $Nb_{70}Zr_{15}Si_{15}$

A. INOUE, S. OKAMOTO*, T. MASUMOTO
The Research Institute for Iron, Steel and Other Metals, and *Graduate School, Tohoku University, Sendai 980, Japan*

H. S. CHEN
Bell Laboratories, 600 Mountain Avenue, Murray Hill, New Jersey 07974, USA

The effect of cold rolling on the superconducting properties was examined for amorphous $Nb_{50}Zr_{35}Si_{15}$ and $Nb_{70}Zr_{15}Si_{15}$ superconductors. Cold rolling to 10 to 20% reduction in thickness results in a rise of superconducting transition temperature (T_c) and a decrease in transition width (ΔT_c), upper critical field gradient near T_c [$-(dH_{c2}/dT)_{T_c}$], critical current density [$J_c(H)$] and normal electrical resistivity (ρ_n). Changes of about 7% for T_c, 33% for ΔT_c, 12% for $-(dH_{c2}/dT)_{T_c}$ and 70% for $J_c(H)$ are found. The rise of T_c upon cold rolling was considered to originate from the increase in the electron–phonon coupling constant (λ) due to an increase in the electronic density of states at the Fermi level [$N(E_f)$] and a decrease in the phonon frequency (ω), while the decreases in ΔT_c, $J_c(H)$ and ρ_n were attributed to the decrease in fluxoid pinning force due to an increase in homogeneity in the amorphous structure. From the results described above, the following two conclusions were derived: (a) cold rolling causes changes in electronic and phonon-states in the quenched amorphous phase, and (b) deformation upon cold rolling occurs not only in the coarse deformation bands observable by optical microscopy, but also on a much finer scale comparable to the coherence length ($\simeq 7.7$ nm).

1. Introduction

Recently, a large flux flow resistivity has been observed for the amorphous superconductors of Zr-based [1, 2], Nb-based [3, 4] and Mo-based [5] alloys produced by the melt-quenching technique. This indicates that the amorphous alloys have a homogeneous structure on the scale of coherence length and are an extremely soft superconductor in which the fluxoid pinning force is very weak. Amorphous alloys were reported to deform very inhomogeneously upon cold rolling. Plastic deformation was generally considered to occur at narrow shear bands separated by intervals of several micrometres [6]. Previous results revealed that cold rolling causes significant changes in a wide range of properties such as sound velocity [7], magnetization behaviour [8], internal friction [9], heat release associated with structural relaxation [10], hardness [11] and corrosion resistance [12]. It was expected that the introduction of such an inhomogeneous strain into the as-quenched amorphous phase would exert a significant effect on the structure-sensitive superconducting properties such as transition temperature T_c, transition width ΔT_c, upper critical field $H_{c2}(T)$, critical current density $J_c(H)$, flux flow resitivity $\rho_f(H)$ and normal electrical resistivity ρ_n. Koch *et al.* [13] examined the effect of cold rolling on the superconducting properties of a $(Mo_{0.6}Ru_{0.4})_{82}B_{18}$ amorphous alloy and reported that inhomogeneous deformation up to 20% reduction in thickness did not change the normal resistivity, T_c or H_{c2}, but did degrade the critical current density. Recently, the present authors reported briefly that all the

0022–2461/84 $03.00 + .12

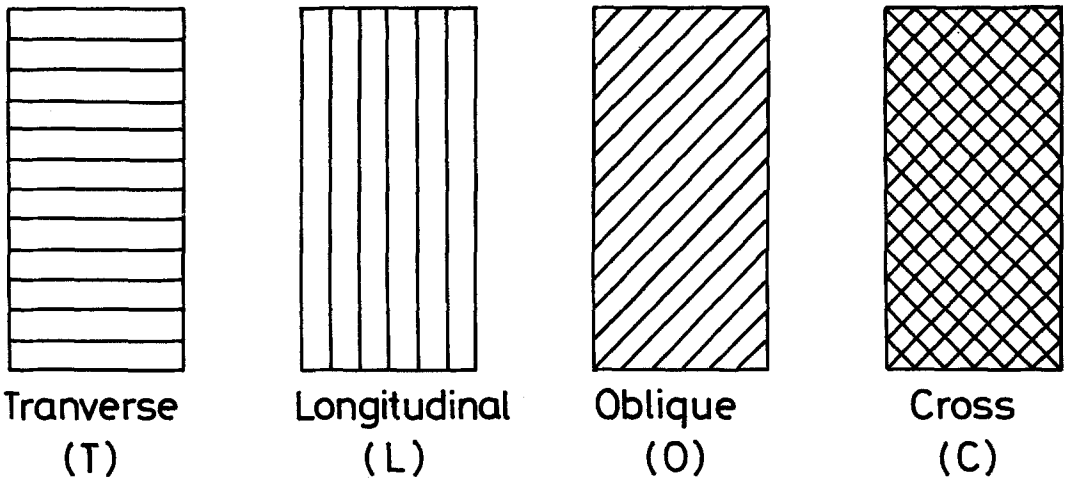

Figure 1 Schematic illustration of deformation bands introduced by cold rolling along different directions against the long axis of ribbon sample, (a) longitudinal, (b) transverse, (c) oblique, and (d) cross.

superconducting properties; T_c, ΔT_c and $H_{c2}(T)$ as well as $J_c(H)$ of an amporphous $Nb_{50}Zr_{35}Si_{15}$ alloy did change definitely upon cold rolling [14]. The aim of this paper is to present further detailed results on the influence of cold rolling on T_c, ΔT_c, $H_{c2}(T)$, $J_c(H)$ and $\rho_f(H)$ behaviours of amorphous alloys, $Nb_{50}Zr_{35}Si_{15}$ and $Nb_{70}Zr_{15}Si_{15}$. The two alloys were chosen because they exhibit typical amorphous-type superconducting properties [3] and are very ductile to sustain a heavy cold rolling [15]. T_c, ΔT_c and $-(dH_{c2}/dT)_{T_c}$ are 3.73 K, 0.15 K and $1.67 \times 10^6 A m^{-1} K^{-1}$ (21.0 kOe K^{-1}) for $Nb_{50}Zr_{35}Si_{15}$ and 4.01 K, 0.15 K and $1.62 \times 10^6 A m^{-1} K^{-1}$ (20.3 kOe K^{-1}) for $Nb_{70}Zr_{15}Si_{15}$, respectively.

2. Experimental methods

Nb–Zr–Si alloys were made from pure elements of niobium, zirconium and silicon and alloyed under a purified and gettered argon atmosphere in an arc furnace on a water-cooled copper mould. Long ribbon specimens were produced by squirting a stream of molten alloy melted with a levitation furnace under argon through a quartz nozzle on a single spinning roller which was rotating at a speed of about 4000 rpm. The ribbons thus produced were typically 20 μm thick and 1 mm wide. The amorphous nature of the quenched samples was confirmed by conventional X-ray diffraction method and transmission electron microscopy. Rolling was carried out at room temperature in a four roller mill with high chromium steel work rolls. The samples were sandwiched between 18Cr–8Ni stainless steel sheets to prevent the initiation of surface cracking and to yield a uniform strain throughout the samples. The rolling was performed systematically along different directions against the long axis of the ribbon samples, i.e. transverse (T), longitudinal (L), oblique (O) and cross (C), as shown schematically in Fig. 1. Hereafter, their rolling directions are designated by T, L, O and C, respectively. The reduction in thickness was determined by measuring the change in sample length because it was rather difficult to measure accurately the change in thickness. Shear bands introduced on the sample surface were revealed with an optical microscope. Deformations of up to 30% reduction in thickness were possible without introducing cracking flaws and pin holes.

Measurements of superconducting and electrical properties, T_c, $H_{c2}(T)$, $J_c(H)$, $\rho_f(H)$ and ρ_n were made resistively using a conventional four-probe technique. The temperature was measured with an accuracy of ± 0.01 K using a calibrated germanium thermometer. The magnetic field up to 7.2×10^6 A m^{-1} (90 kOe) was applied perpendicularly to the specimen surface and feed current.

3. Results

3.1. Deformation structure

Fig. 2 shows deformation markings on the surfaces and sides of cold-rolled $Nb_{50}Zr_{35}Si_{15}$ amorphous alloy with varying reduction in thickness. With increasing degree of cold rolling, e.g. the reduction in thickness, R, from 10 to 30%, the average density of shear bands increases and the spacing among shear bands decreases monotonically but

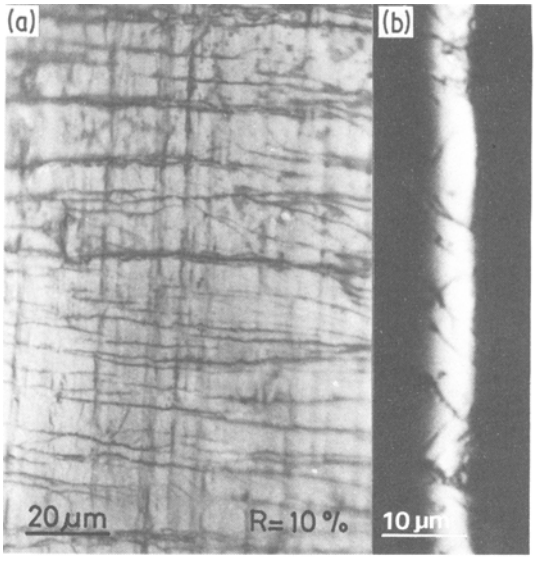

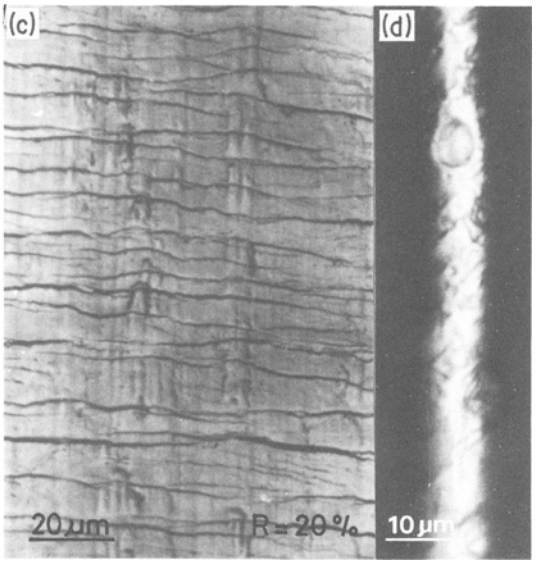

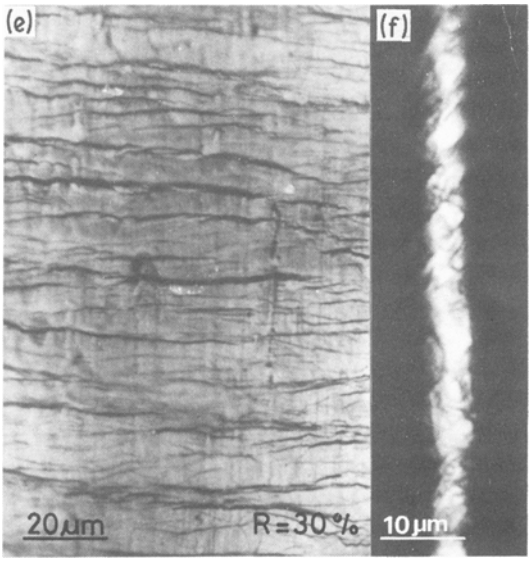

Figure 2 Optical micrographs showing the deformation markings on the surfaces and sides of an amorphous $Nb_{50}Zr_{35}Si_{15}$ alloy cold-rolled to different reductions in thickness along the transverse direction (a and b) $R = 10\%$, (c and d) $R = 20\%$, and (e and f) $R = 30\%$.

not linearly, because further plastic deformation occurs in the previously deformed region as well as in undeformed regions in which new shear bands have been created. It is noted that the shear bands intersect each other and the frequency of the intersection tends to increase with increasing R. Fig. 3 shows the deformation markings on the surfaces of the $Nb_{50}Zr_{35}Si_{15}$ samples cold-rolled to 30% reduction in thickness along L, T, O and C directions. The patterns of deformation marking are very similar to those illustrated schematically in Fig. 1. Various types of deformation markings thus can be induced by simply changing the rolling direction.

3.2. Change in electrical resistivity at 4.2 K

Fig. 4 shows the change in electrical resistivity ρ_n at 4.2 K for $Nb_{50}Zr_{35}Si_{15}$ alloy as a function of R. Although the accuracy of absolute ρ_n measurements is 10 to 20% owing to the difficulty of accurate measurement of cross-section, the tendency that, ρ_n decreases initially, shows a minimum at $R \simeq 20\%$ and then increases with further increasing reduction in thickness is clearly seen. The decrease in ρ_n is about twice larger for the "cross" and "oblique" samples than for the "longitudinal" sample. The maximum change in ρ_n is about 30% for the former two samples.

3.3. Changes in superconducting properties

Fig. 5 shows the change in the electrical resistance curves in the vicinity of T_c for the $Nb_{50}Zr_{35}Si_{15}$ amorphous alloy upon cold rolling. In all cases, T_c increases upon cold rolling. The rise in T_c is correlated with the decrease in ρ_n, with the exception for the case of O-10% sample. T_c and ΔT_c of the $Nb_{50}Zr_{35}Si_{15}$ and $Nb_{70}Zr_{15}Si_{15}$ alloys are plotted as a function of R in Figs. 6 and 7, respectively. T_c is the temperature corresponding to $R/R_n = 0.5$, where R_n is the resistance in the normal state. The transition width ΔT_c is defined as the temperature interval between 0.1 and 0.9

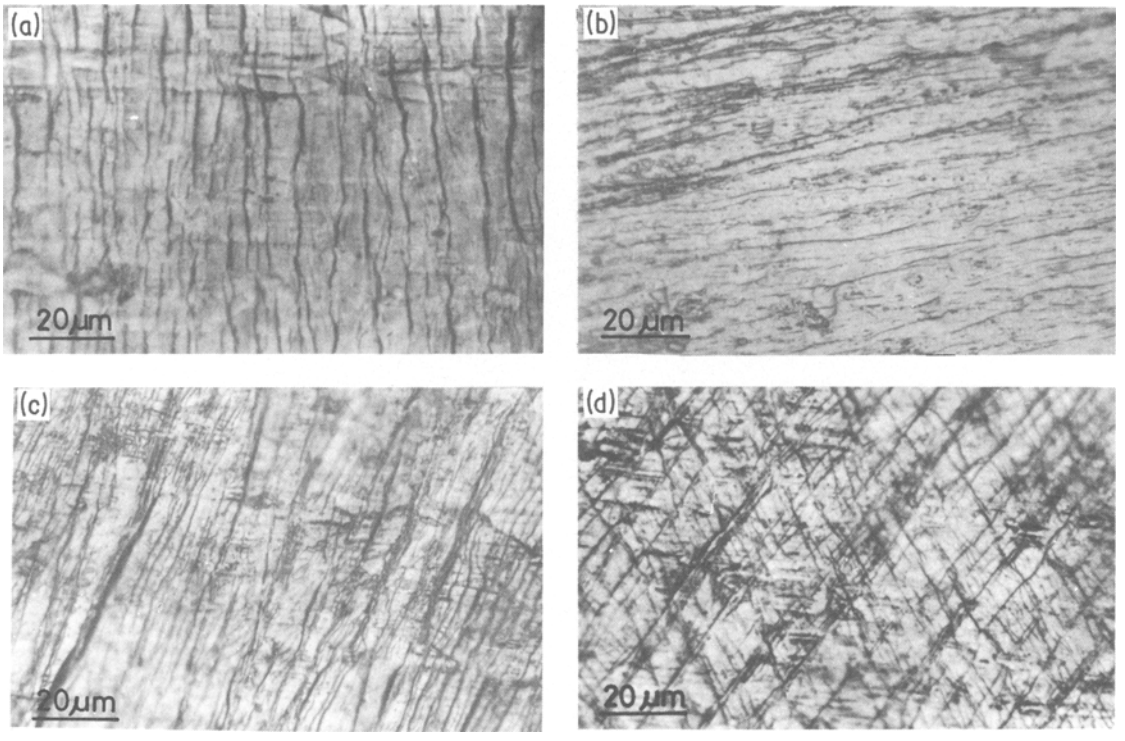

Figure 3 Optical mocrographs showing the deformation markings on the surfaces of an amorphous $Nb_{50}Zr_{35}Si_{15}$ alloy cold-rolled to 30% reduction in thickness along the T, L, O and C directions.

R/R_n. Upon cold rolling, T_c of the $Nb_{50}Zr_{35}Si_{15}$ alloy (3.73 K at $R = 0\%$) increases and shows maximum value at $R = 10\%$ for the "oblique" sample and at $R = 20\%$ for the "longitudinal" and "cross" samples. The largest rise of T_c is 0.27 K for the O-10% sample. On the other hand, the $Nb_{70}Zr_{15}Si_{15}$ alloy exhibits a monotonous rise of T_c with increasing R. The trend of the rise of T_c

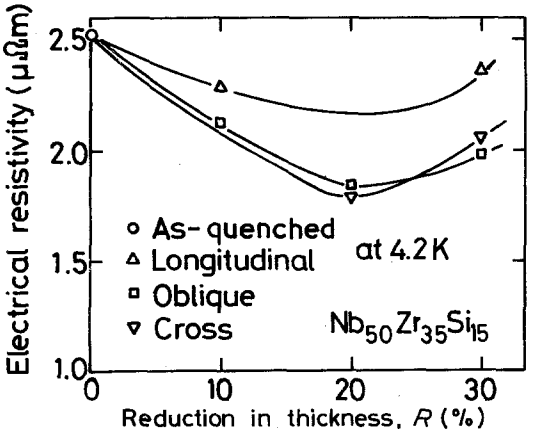

Figure 4 Change in normal electrical resistivity at 4.2 K of an amorphous $Nb_{50}Zr_{35}Si_{15}$ alloy with reduction in thickness along the L, O and C directions.

against reduction in thickness is different between the two alloys, but as it is seen in Figs. 6 and 7, both alloys show ΔT_c decreasing monotonically with increasing R. The decrease in ΔT_c is larger for the "cross" sample than for the "oblique" sample. The change is large and is about 33% for the C-30% samples for $Nb_{50}Zr_{35}Si_{15}$ and $Nb_{70}Zr_{15}Si_{15}$ alloys. The decrease in ΔT_c suggests that the amorphous structure becomes more homogeneous on the scale of coherence length (7.5 to 7.6 nm) upon cold rolling.

H_{c2} values of $Nb_{50}Zr_{35}Si_{15}$ alloy cold-rolled to 20% and 30% reduction in thickness, R, are plotted as a function of temperature in Figs. 8 and 9. The solid lines in the figures represent a linear extrapolation near T_c. All the samples, as quenched and cold rolled, show a linear relationship between H_{c2} and temperature in the temperature range near T_c. The H_{c2} gradient near T_c $(-dH_{c2}/dT)_{T_c}$ for amorphous $Nb_{50}Zr_{35}Si_{15}$ and $Nb_{70}Zr_{15}Si_{15}$ alloys as a function of reduction in thickness is shown in Fig. 10. With increasing reduction in thickness, the gradient values decrease initially, exhibit minimum values at $R \simeq 20\%$ and then tend to increase. The decrease appears to increase

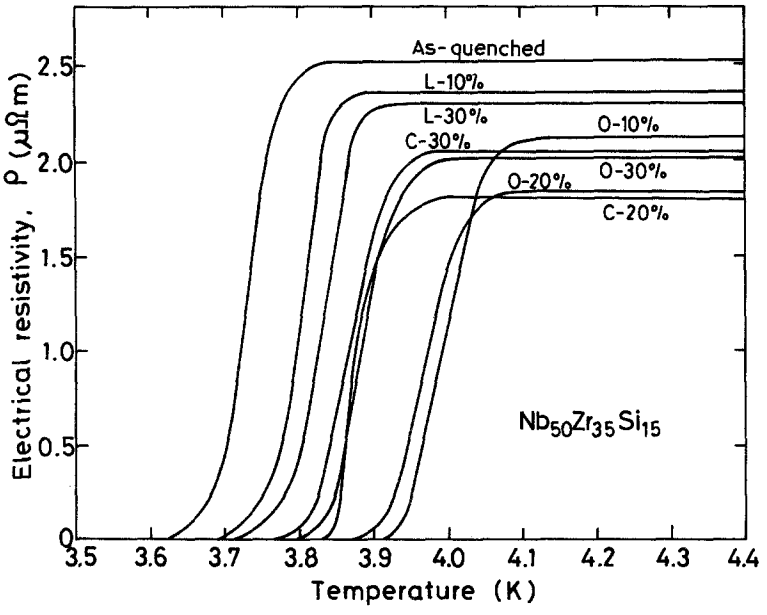

Figure 5 Electrical resistivity near T_c for an amorphous $Nb_{50}Zr_{35}Si_{15}$ alloy cold-rolled to 10, 20 and 30% reductions in thickness along the L, O and C directions.

in the order of longitudinal > oblique > cross and the decreasing ratio of the L-30% sample reaches about 12%.

3.4. Changes in critical current density $J_c(H)$ and flux flow resistivity $\rho_f(H)$

Fig. 11 shows $J_c(H)$ at $\simeq 1.40$ K and 2.60 K as a function of magnetic field, H, for the $Nb_{50}Zr_{35}Si_{15}$ amorphous alloy in the as-quenched and cold-rolled (C-30%) states. The $J_c(H)$ is considerably lower for the rolled sample than for the as-quenched sample over the whole region except the field just below H_{c2}. This indicates that the fluxoid pinning force becomes weaker upon cold rolling, The rolled sample exhibits a "peak effect" near H_{c2} which is absent in the as-quenched sample and the $J_c(H)$ values near H_{c2} are higher for the rolled sample owing to the peak effect.

Fig. 12 shows the normalized flux flow resistivity ρ_f/ρ_n as a function of magnetic field for the $Nb_{50}Zr_{35}Si_{15}$ alloy in the as-quenched and cold-rolled (C-30%) states. We define the flux flow resistivity ρ_f as a linear gradient dV/dI above the

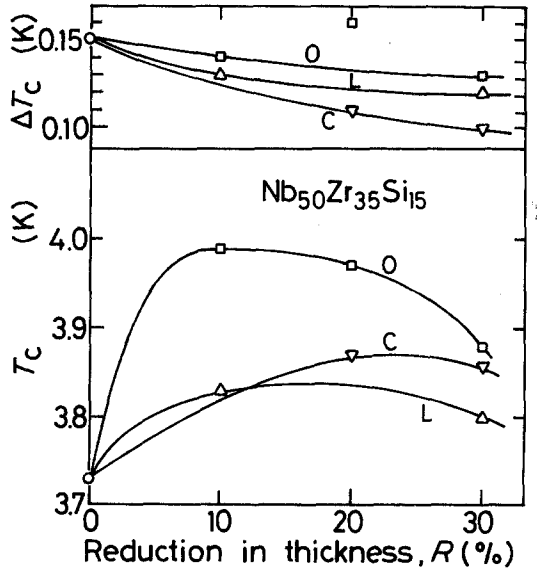

Figure 6 Changes in the superconducting transition temperature (T_c) and the transition width (ΔT_c) of an amorphous $Nb_{50}Zr_{35}Si_{15}$ alloy with reduction in thickness along the L, O and C directions.

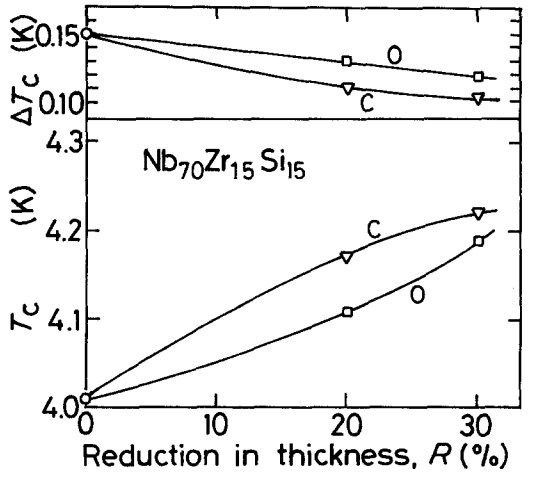

Figure 7 Changes in the superconducting transition temperature (T_c) and the transition width (ΔT_c) of an amorphous $Nb_{70}Zr_{15}Si_{15}$ alloy with reduction in thickness along the O and C directions.

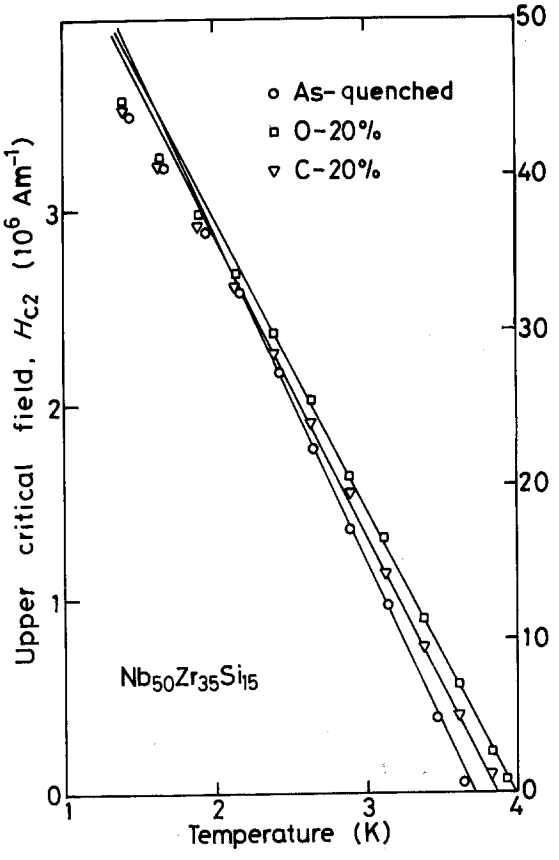

Figure 8 Upper critical field H_{c_2} at various temperatures of an amorphous $Nb_{50}Zr_{35}Si_{15}$ alloy cold-rolled to 20% reduction in thickness along the L, O and C directions.

depinning current density on the current–voltage (I–V) curve measured in constant magnetic fields. The linear part in the relation of ρ_f/ρ_n against H extends to a high magnetic field for the cold-rolled sample. The arrows in the figure represent the H_{c2} values. H_{c2} values at both the temperatures of 1.4 and 2.6 K increase upon cold rolling, in agreement with the result shown in Fig. 9. A reflection point on the ρ_f/ρ_n–H curve at 1.39 K corresponding to the peak effect is seen for the rolled sample.

4. Discussion

4.1. Changes in T_c and ΔT_c

As shown in Figs. 6 to 9, the cold rolling results in a rise in T_c and a decrease in ΔT_c and $-(dH_{c2}/dT)_{T_c}$. Considering the fact that these superconducting characteristics are very structure-sensitive, the above described changes upon cold rolling suggest that cold rolling alters the electronic- and phono-states in amorphous phase. In general, the change in ΔT_c is attributed to the variation of the homogeneity in the amorphous phase on the scale of coherence length (ξ). The Ginzburg–Landau coherence length at 0 K, $\xi_{GL}(0)$, is estimated from the measured values of T_c and $-(dH_{c2}/dT)_{T_c}$ by using the following equation [16].

$$\xi_{GL}(0) = \left[\frac{\phi_0}{2\pi T_c}\left(-\frac{dH_{c2}}{dT}\right)_{T_c}^{-1}\right]^{1/2} \quad (1)$$

where ϕ_0 is the flux quantum. The $\xi_{GL}(0)$ of $Nb_{50}Zr_{35}Si_{15}$ alloy in the cold-rolled (C-30%) state thus estimated is about 7.7 nm. The decrease in ΔT_c upon cold rolling indicates that the amorphous phase becomes more homogeneous on the scale of coherence length ($\simeq$ 7.7 nm). The spacing among shear bands ($\simeq$ 0.5 to 1.0 μm) (see Fig. 2) are much larger than the $\xi_{GL}(0)$ value. This suggests that the microscopic change in the quenched-in structure upon cold rolling occurs in the regions between the shear bands as well as on shear bands.

We shall consider the microscopic origin of the rise of T_c upon cold rolling. According to the McMillan's theory [17] which is applicable to an intermediately strong-coupled superconductor, T_c is related to the Debye temperature (θ_D) and the electron–phonon coupling constant (λ) by the following expression,

$$T_c = \frac{\theta_D}{1.45}\exp\left[\frac{-1.04(1+\lambda)}{\lambda-\mu^*(1+0.62\lambda)}\right] \quad (2)$$

where μ^* is the Coulomb pseudopotential and can be approximated to be 0.13 for the $(Nb–Zr)_{85}Si_{15}$ amorphous alloys based on the data [18] of transition metal-based crystalline superconductors. λ is expressed as,

$$\lambda = 2\int_0^\infty \alpha^2(\omega)F(\omega)d\omega/\omega = \frac{N(E_f)\langle g^2\rangle}{M\langle\omega^2\rangle} \quad (3)$$

where $\alpha(\omega)$ is the electron–phonon matrix element, $F(\omega)$ is the phonon spectrum, $N(E_f)$ is the electronic bare density of states at the Fermi level, $\langle g^2\rangle$ is the average over the Fermi surface of the square of the electronic matrix element, M is the average ionic mass and $\langle\omega^2\rangle$ is an average of the square of the phonon frequency. Equations 2 and 3 show that the larger are θ_D, λ and $N(E_f)$, and lower is $\langle\omega^2\rangle$, the higher is T_c. There are no actually measured data on the θ_D and $\langle\omega^2\rangle$ of the as-quenched and cold-rolled $(Nb–Zr)_{85}Si_{15}$ amorphous alloys. However, it has been reported

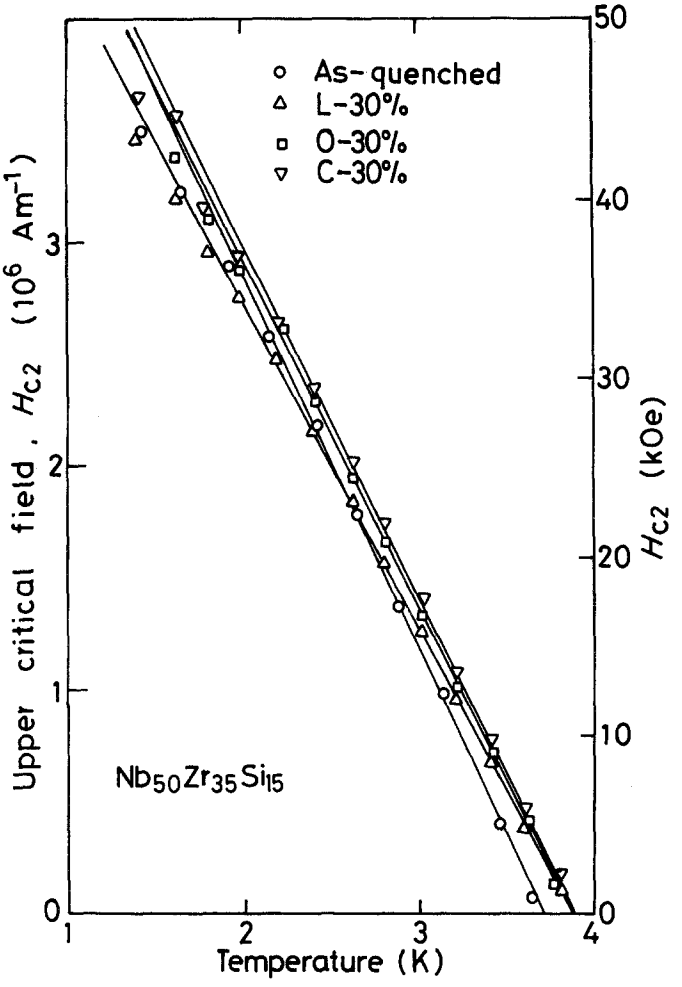

Figure 9 Upper critical field H_{c2} at various temperatures of an amorphous $Nb_{50}Zr_{35}Si_{15}$ alloy cold-rolled to 30% reduction in thickness along the L and C directions.

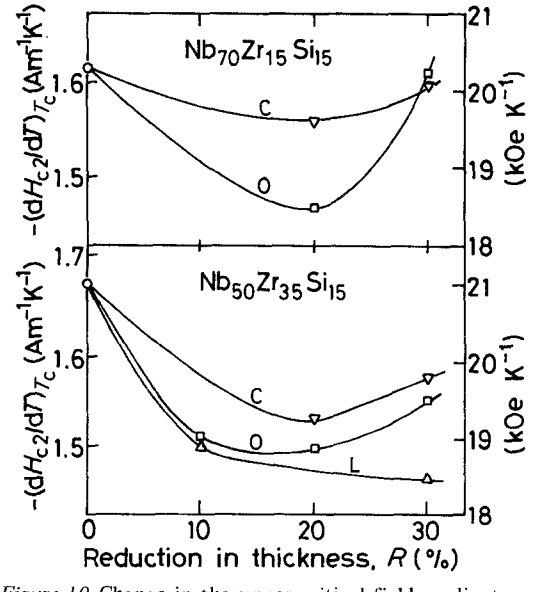

Figure 10 Change in the upper critical field gradient near T_c, $-(dH_{c2}/dT)_{T_c}$, of amorphous $Nb_{50}Zr_{35}Si_{15}$ and $Nb_{70}Zr_{15}Si_{15}$ alloys with reduction in thickness along the L, O and C directions.

for Pd-based [7, 19] and Fe-based and Co-based [20] amorphous alloys that the Young's modulus sound velocity (V_E) decreases by about 6% upon cold rolling or cold drawing. Debye approximation [21] related V_E to the Debye phenon frequency (ω_D) and θ_D by the following expression,

$$V_E = \omega_D \left[\frac{6\pi^2 N}{\Omega}\right]^{-1/3} = \frac{k_B \theta_D}{\hbar}\left[\frac{6\pi^2 N}{\Omega}\right]^{-1/3} \quad (4)$$

where N/Ω is the atomic number per unit volume. Thus θ_D decreases upon cold rolling. Accordingly (see Equation 2), the rise of T_c by cold rolling should arise mainly from an increase in λ and $N(E_f)$ and a decrease in $\langle\omega^2\rangle$ (see Equation 3). The dressed density of states $N(E_f)(1 + \lambda)$ can be calculated from the measured values of ρ_n and $-(dH_{c2}/dT)_{T_c}$ by using the following equation based on the GLAG theories [16].

$$N(E_f)(1 + \lambda) = -\frac{\pi}{8k_B e\rho_n}\left(\frac{dH_{c2}}{dT}\right)_{T_c} \quad (5)$$

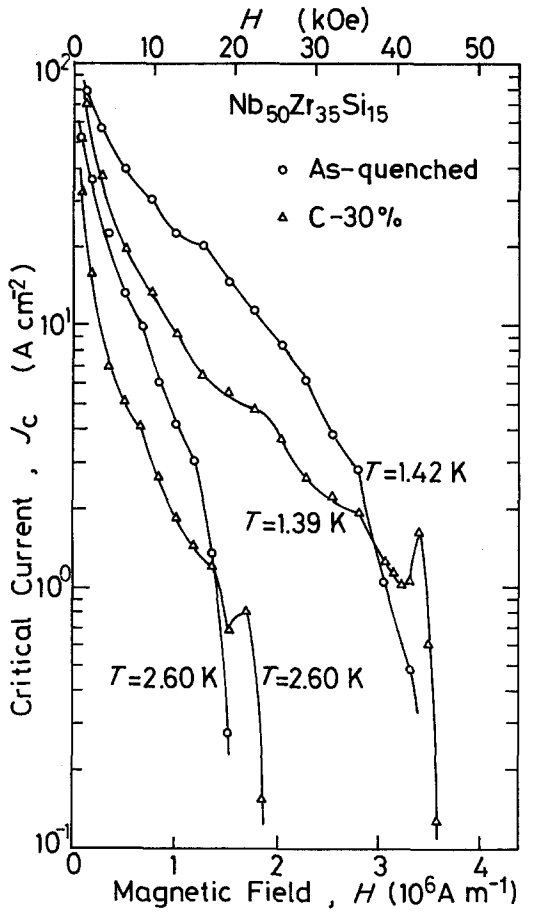

Figure 11 Critical current density, $J_c(H)$, as a function of magnetic field for an amorphous $Nb_{50}Zr_{35}Si_{15}$ alloy in as-quenched and 30% cold-rolled states.

Fig. 13 shows the change in $N(E_f)(1 + \lambda)$ of the amorphous $Nb_{50}Zr_{35}Si_{15}$ alloy with reduction in thickness. As seen in the figure, the $N(E_f)(1 + \lambda)$ value tends to increase with increasing reduction in thickness, suggesting that the rise of T_c upon cold rolling is indeed due to the increase in λ and/or $N(E_f)$. The electronic- and phonon-states in the amorphous phase are indeed altered by cold rolling.

In the following the effect of cold rolling on the Ginzburg–Landau parameter (κ), the penetration depth of external field at 0 K (λ_0) and electronic diffusivity (D), which are parameters characterizing the superconductor, were investigated by using the GLAG theories [16], which are applicable to the "dirty" type-II superconductor. The estimation of these parameters was made from the following equations.

$$\kappa = 7.49 \times 10^3 \gamma^{1/2} \rho_n \quad (6)$$

$$\lambda_0 = 1.05 \times 10^{-2} (\rho_n / T_c)^{1/2} \quad (7)$$

$$D = \frac{4 k_B c}{e} \left(- \frac{dH_{c2}}{dT} \right)^{-1}_{T_c} \quad (8)$$

The parameter γ in Equation 6 is the electronic specific heat coefficient and was obtained from the following equation [16].

$$\gamma = - \frac{\pi^3 k_B}{12 e \rho_n} \left(\frac{dH_{c2}}{dT} \right)_{T_c} \quad (9)$$

The changes in κ, λ_0 and D values of the $Nb_{50}Zr_{35}Si_{15}$ amorphous alloy as a function of reduction in thickness are shown in Fig. 14. With increasing reduction in thickness, the values of κ and λ_0 decrease at first, show minimum values at $R = 20\%$ and then increase. On the other hand, the D value increases at first and exhibits a maximum value at $R = 20\%$. Thus, the cold rolling results in a decrease in the dirtiness and an increase in the electronic diffusivity, indicating that the structural homogeneity of the amorphous superconductor enhances by cold rolling. This is consistent with the significant decrease in $J_c(H)$ upon cold rolling.

4.2. Changes in $J_c(H)$ and $\rho_f(H)$

As shown in Fig. 11, the cold rolling causes a significant change in $J_c(H)$. The main change is summarized as follows; (a) the $J_c(H)$ degrades and the fluxoid pinning force becomes weak, and (b) a clear peak effect appears near H_{c2}. Such changes are reasonably interpreted with the assumption that the amorphous phase changed into a more homogeneous state upon rolling, being consistent with the conclusion derived from the data of ρ_n, ΔT_c, κ and D. The degradation of $J_c(H)$ by cold rolling was also reported for an amorphous $(Mo_{0.6}Ru_{0.4})_{82}B_{18}$ alloy by Koch *et al.* [13]. The reason why cold rolling causes the significant increase in the homogeneity in the amorphous phase is unknown. It is clear, however, that shear bands introduced by cold rolling do not act as effective fluxoid pinning centres.

There is no established interpretation and theory on the reason for the appearance of peak effect. However, considering the fact that the appearance of the peak effect is more evident for the amorphous superconductors exhibiting lower $J_c(H)$ values [1] and for cold-rolled amorphous superconductors, the appearance of the peak effect upon cold rolling may be interpreted as follows; the fluxoid pinning force in the matrix

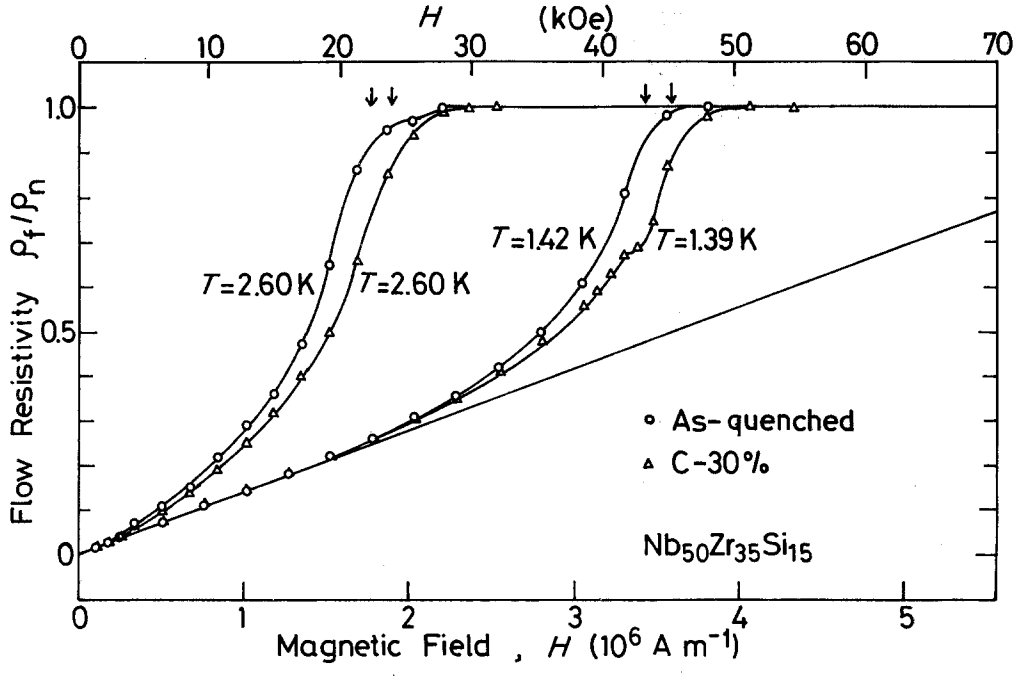

Figure 12 Normalized flux flow resistivity ρ_f/ρ_n as a function of magnetic field for an amorphous $Nb_{50}Zr_{35}Si_{15}$ alloy in as-quenched and 30% cold-rolled states.

phase becomes weak upon cold rolling and hence the contribution of the surface pinning effect to the total fluxoid pinning force increases for the cold-rolled samples exhibiting a large surface ruggedness, resulting in the appearance of the peak effect.

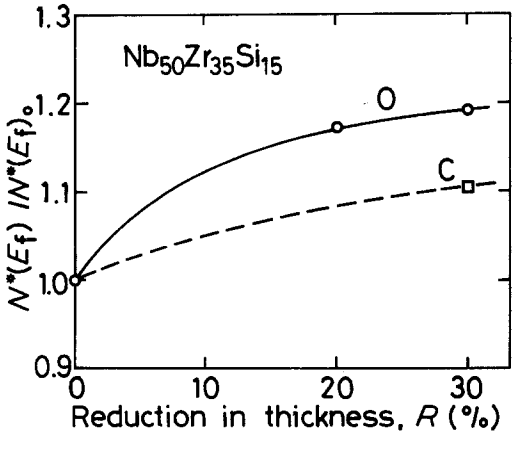

Figure 13 Change in the electronic dressed density of states at the Fermi level $N^*(E_f) = N(E_f)(1 + \lambda)$ of an amorphous $Nb_{50}Zr_{35}Si_{15}$ alloy with reduction in thickness along the O and C directions.

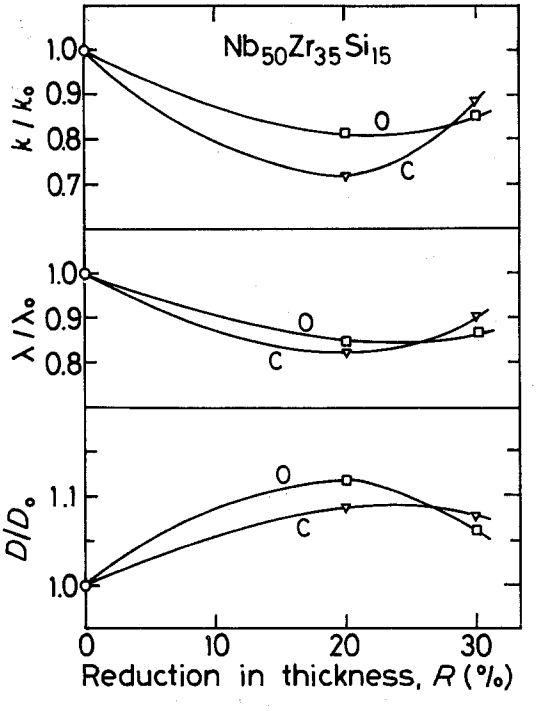

Figure 14 Changes in the Ginzburg–Landau parameters κ, the penetration length λ_0 and the electronic diffusivity D of an amorphous $Nb_{50}Zr_{35}Si_{15}$ alloy with reduction in thickness along the O and C directions.

4.3. Change in the superconducting properties with rolling directions

As is evident from the results shown in Section 3, all the superconducting properties measured in the present work changed appreciably upon cold rolling. However, no systematic difference in the change in the superconducting properties against the rolling direction was observed, despite the fact that the frequency of the intersections of shear bands is much higher for the "cross" sample than for the samples cold-rolled to the other directions. This indicates that the changes in the superconducting properties upon cold rolling are affected little by the presence of shear bands, which are observable with an optical microscope, but originate from the local atomic rearrangement in the bulk on the scale much shorter than the shear band interspacings (0.5 to 1.0 μm).

5. Summary

The effect of cold rolling on the superconducting properties of an amorphous phase was examined for $Nb_{50}Zr_{35}Si_{15}$ and $Nb_{70}Zr_{15}Si_{15}$ amorphous ribbons produced by the melt-spinning technique. The results obtained are summarized as follows:

1. T_c increases with cold rolling. A large increase in T_c of 0.27 K is seen. The rise of T_c is attributed to the increase in λ due to the increase in $N(E_f)$ and the decrease in $\langle\omega^2\rangle$.

2. ΔT_c decreases monotonically with increasing reduction in thickness and the largest decreasing ratio is about 33%. From the significant reduction of ΔT_c, it is suggested that the deformation of amorphous phase by cold rolling occurs not only in the shear band regions, which are distinguishable by optical microscopy, but also in the bulk within the scale of coherence length ($\simeq$ 7.7 nm), which is much smaller than the spacings among shear bands.

3. The $J_c(H)$ degrades significantly upon cold rolling and a peak effect appears near H_{c2}. Such changes in the $J_c(H)$ behaviour are considered to originate from the degradation of the fluxoid pinning force due to the enhancement of homogeneiety in the amorphous structure upon cold rolling. The increase in the homogeneity in the amourphous phase upon cold rolling is also supported from the results that the values of ΔT_c, κ and ρ_n decrease and the D value increases.

References

1. N. TOYOTA, T. FUKASE, A. INOUE, Y. TAKAHASHI and T. MASUMOTO, *Physica* **107B** (1981) 465.
2. A. INOUE, Y. TAKAHASHI, N. TOYOTA, T. FUKASE and T. MASUMOTO, *J. Mater. Sci.* **17** (1982) 3299.
3. A. INOUE, Y. TAKAHASHI, N. TOYOTA, T. FUKASE and T. MASUMOTO, *ibid.* **18** (1983) 114.
4. A. INOUE, Y. TAKAHASHI, N. TOYOTA, T. FUKASE and T. MASUMOTO, *Trans. Jpn. Inst. Met.* **23** (1982) 693.
5. A. INOUE, S. OKAMOTO, N. TOYOTA, T. FUKASE and T. MASUMOTO, unpublished research (1982).
6. H. S. CHEN, *Rep. Prog. Phys.* **43** (1980) 353.
7. H. S. CHEN, *Scripta Metall.* **9** (1975) 411.
8. F. R. LUBORSKY, J. L. WALTER and D. G. LEGRAND, *IEEE Trans. Mag.* **MAG-12** (1980) 930.
9. M. BARMATZ, K. W. WYATT and H. S. CHEN, Proceedings of the 2nd International Conference on Rapidly Quenched Metals Cambridge, November 1975 (MIT Press, Cambridge, 1976) p. 431.
10. H. S. CHEN, *Appl. Phys. Lett.* **29** (1976) 328.
11. M. HAGIWARA, private communication, Unitika Research Development Center, Unitika Ltd., Uji 611, Japan (1982).
12. C. A. PAMPILLO and H. S. CHEN, *Mater. Sci. Eng.* **13** (1974) 181.
13. C. C. KOCH, I. O. SCARBROUGH, D. M. KROEGER and A. DASGUPTA, *Appl. Phys. Lett.* **37** (1980) 451.
14. A. INOUE, S. OKAMOTO, T. MASUMOTO and H. S. CHEN, *Scripta Metall.* **16** (1982) 1393.
15. A. INOUE, Y. TAKAHASHI, C. SURYANARAYANA and T. MASUMOTO, *J. Mater. Sci.* **17** (1982) 3253.
16. T. R. ORLANDO, E. J. McNIFF Jr, S. FORNER and M. R. BEASLEY, *Phys. Rev. B* **19** (1979) 4545.
17. W. L. McMILLAN, *Phys. Rev.* **167** (1968) 331.
18. K. B. BENNEMANN and J. W. GARLAND, in "Superconductivity in d- and f-Band Metals", edited by D. H. Douglass, AIP Conference Proceedings No. 4 (AIP, New York, 1972) p. 116.
19. A. INOUE, H. S. CHEN, J. T. KRAUSE and T. MASUMOTO, *LAM 5* (1983) to be published.
20. H. S. CHEN, R. C. SHERWOOD, S. JIN, G. C. CHI, A. INOUE, T. MASUMOTO and M. HAGIWARA, *29 MMM* (1983) to be published.
21. T. OTSUKA, "Ferroelectrics and Superconductor" (The Japan Inst. Metals, Sendai, 1973) p. 131.

Received 27 June
and accepted 26 July 1983